The influence of resistance drift on measurements of the activation energy of conduction for phase-change material in random access memory line cells

J. L. M. Oosthoek,[1,a)] D. Krebs,[2] M. Salinga,[3] D. J. Gravesteijn,[4] G. A. M. Hurkx,[4] and B. J. Kooi[1]
[1]*Zernike Institute for Advanced Materials, Materials innovation institute M2i, University of Groningen, Nijenborgh 4, 9747 AG Groningen, The Netherlands*
[2]*IBM Zurich Research Laboratory, Saeumerstr. 4, CH-8803 Rueschlikon, Switzerland*
[3]*I. Physikalisches Institut IA, RWTH Aachen, Sommerfeldstrasse 14, 52074 Aachen, Germany*
[4]*NXP Semiconductors, Kapeldreef 75, 3001 Leuven, Belgium*

(Received 31 July 2012; accepted 19 September 2012; published online 18 October 2012)

Temporal drift of the amorphous resistance in phase-change random access memory (PRAM) is a temperature accelerated process. Increasing the temperature will speed up the drift process which is shown to affect measurements of the activation energy of conduction (Ea, slope of log(R) versus 1/kT). Doped SbTe phase change (PRAM) line cells were brought to the amorphous state and were subjected to annealing experiments. First, it is shown that when the temperature is increased by a fixed rate, the resistance does not follow a unique function of temperature but depends on the heating rate. This can be attributed to resistance drift taking place during the ramp. Upon cooling, the drift process freezes and only then physically relevant, i.e., time independent, values for Ea can be obtained, because of the absence of additional drift. The observed increase in resistance as a function of annealing history (for various frozen-in drift levels) is modeled and well-reproduced using a trap limited band transport model. The model explains these observations by an increase of the temperature dependent band gap by about 47 meV due to drift at 418 K. © *2012 American Institute of Physics*. [http://dx.doi.org/10.1063/1.4759239]

I. INTRODUCTION

Phase change random access memory (PRAM) is one of the most promising candidates for the next-generation of non-volatile memories.[1] A well-known and important phenomenon found in PRAM in general is that the amorphous resistance is not stable in time.[2] After a cell is brought to the amorphous state (e.g., by applying a RESET pulse), the resistance drifts (increases) as a function of time by a power law when kept at a constant temperature. Values for the power law exponent vary for different cell types (also meaning geometrically identical cells with the same phase-change material but produced by different methods) typically between 0.04 and 0.1.[2–8] Resistance drift is not necessarily a problem for a memory based on two distinct stable states, since (in the absence of crystallization) the contrast between the states improves in time. However, multilevel memory applications are based on programming the cell to different amorphous states[9,10] with resistances in the whole range of typically three orders of magnitude between the fully crystalline and maximally amorphous state. Here, the resistance drift poses the danger of one state drifting into the resistance window of the next state.

Furthermore, resistance drift is a temperature accelerated process.[7,11,12] Increasing the temperature will speed up the drift process. This process of drift qualitatively shows similar behavior at a large range of temperatures.[11] Therefore, when performing temperature dependent measurements on amorphous cell properties, the effect of drift has to be taken into account. One important parameter is the activation energy of conduction E_A[2,13,14] of the amorphous phase. In the simplest model of a single carrier semiconductor[1] (p-type here[15]), E_A can be linked to the difference between the valence band and the Fermi energy level for hole conduction[2,8] and is about half the value of the band gap.[2,16] E_A is commonly obtained directly from the slope of the (natural logarithm of the) resistance R as a function of temperature T (i.e., log(R) versus 1/kT where k is Boltzmann constant) and thus provides information on the band gap of the amorphous phase.

In the literature, an increase of E_A with drift was reported.[2,8,12,17,18] Two studies[2,8] were based on direct measurements obtained from the resistance data. One of these studies[2] reported an increase of E_A from 0.22 eV as determined directly after RESET to 0.38 eV after annealing at 443 K. Another study[8] reported that the activation energy measured after annealing at a temperature of 363 K increased by 40 meV after subsequently annealing at 403 K. Furthermore, the increase in activation energy upon drift has been related to an increase in the optical band gap.[12]

In order to measure the activation energy from resistance data, care must be taken to properly separate the effect of temporal drift from the regular negative temperature dependence.[2,8,13] In this paper, it will become clear that the activation energy of conduction cannot be obtained from the slope of the resistance versus temperature data by directly heating the cell after RESET as has been done regularly in previous works. It will be shown that when drift occurs during the measurement, a lower value of the slope of log(R) versus 1/kT will be found during heating. Therefore, any

a)Corresponding author: jasper.l.m.oosthoek@gmail.com.

apparent increase of the slope with drift will appear to overshadow the actual physically relevant increase of E_A. Furthermore, it is shown that even in the absence of (additional) drift, the temperature dependence of the band gap, and thus the activation energy, has to be taken into account.

II. EXPERIMENTAL

PRAM line cells with dimensions $700(\pm 10) \times 340(\pm 40) \times 20\ nm^3$ were produced by optical lithography; details can be found in Ref. 15. The cells were switched with a Tektronix AFG3102 arbitrary function generator allowing for 50 ns RESET pulses with 3 ns edges. The cell resistance was measured with a Keithley 2600 source meter at 0.1 V. More information of the measurement setup can be found in Ref. 3. The cell temperature was accurately controlled with a PID controller and a linear power supply connected to a heating filament located close to the cell. Cooling was performed passively by switching off the power supply. To reach temperatures below room temperature (298 K), the stage is connected thermally to a liquid nitrogen reservoir by a ~50 cm copper heat conductor.

III. RESULTS

In a first experiment, a PRAM line cell was switched to the amorphous state and the resistance was subsequently measured as a function of time (Fig. 1(a)). Note the excellent reproducibility when this measurement is repeated after various annealing histories. The resistance follows the well-established power law behavior[2] $R = R_0 \cdot (t/t_0)^{\alpha}$ with $\alpha = 0.081$. 1000 s after RESET, the temperature was increased by a fixed ramp rate until the cell crystallized (resistance dropped below 10 kΩ). As the phase-change material is of a fast growth type, the crystallization behavior is characterized by a sharp drop in resistance[19] when two crystal growth fronts meet.[19] Since this study mainly focuses on drift, the final crystallization is not shown in Fig. 1(b) to aid readability. After cooling back to 298 K, the cell was fully crystallized by a SET pulse to crystallize any remaining amorphous regions. The experiment was performed for a wide range of ramp rates (15, 8, 4, 2, 1, 0.5 K/min). The resistance curves are plotted in Fig. 1(b) as a function of 1/kT.

Fig. 1(b) clearly shows that the measured amorphous resistance is not a unique function of the temperature. Although the resistance curves during the temperature ramp all start from the same point R_S at 298 K, the curves diverge as the temperature is increased. This is quantified in the inset of Figure 1(b) where the slope of log(R) versus 1/kT is calculated from the start of the ramp. The slope has been identified with the activation energy of conduction.[2,13,14] The obtained values of the slope at the start of the ramp range vary between 0.17 eV and 0.24 eV. It is considered to be highly unlikely that the band gap differs with a factor of 1.4, while the resistance and its drift measured only seconds before at 298 K was completely reproducible.

Above 333 K, the slopes of all curves are equal to about 0.17 eV. The resistance values of the slowest ramp at a given temperature remain a factor of two higher than the resistance values measured during the fastest ramp at the same temperature. This can be explained by the lower ramp rates taking longer to reach a given temperature allowing for more drift and thus leading to a higher cell resistance. Clearly, the reversible temperature dependence and the irreversible drift are entangled in this measurement. In the following, we will present data in which the two contributions to the resistance will be separated.

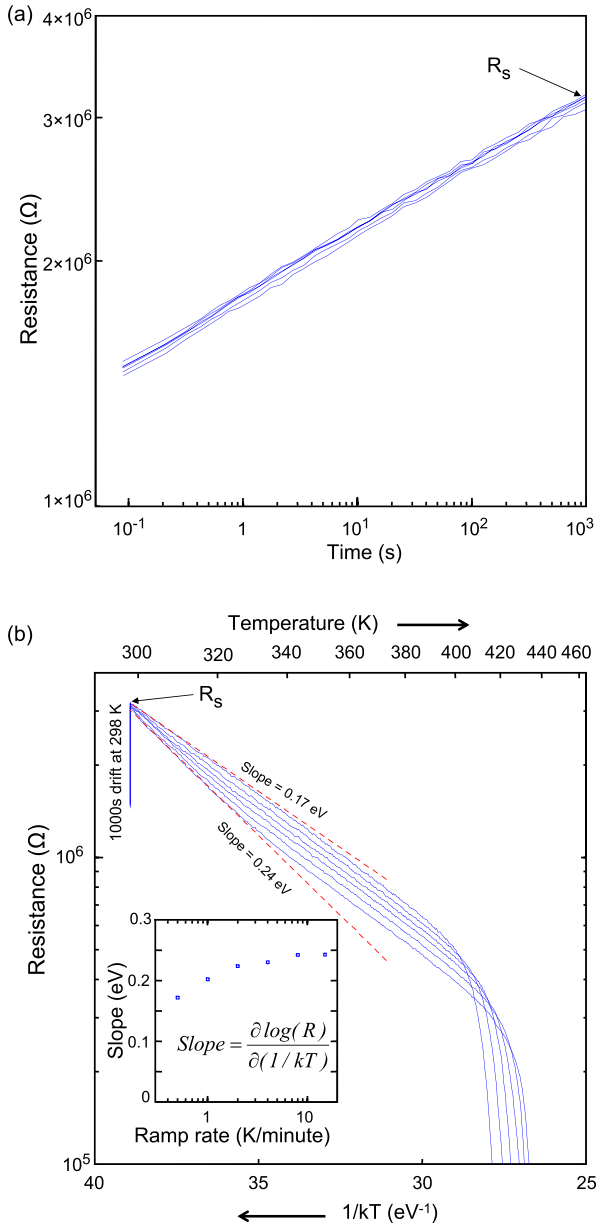

FIG. 1. (a) After RESET, the cell resistance was measured as a function of time for 1000 s. (b) 1000 s after RESET, the temperature was increased with a constant ramp rate until the cell crystallized. This was repeated for a wide range of ramp rates (15, 8, 4, 2, 1, 0.5 K/min). The x-axis has been reversed so the cell temperature increases to the right. The slope of the resistance versus 1/kT (obtained from the data below 333 K) depends on the ramp rate (see inset).

The question is now which one, or if any, of the measurements of the slope can in fact be interpreted as physically relevant measurement of the activation energy of conduction. The answer is given below and would correspond to heating with the highest possible ramp rate (i.e., close to 0.24 eV),

but it has to be emphasized that this is not a reliable procedure; a reliable method is outlined below.

Fig. 2(a) shows the cell resistance as a function of temperature for a single temperature ramp (10 K/min) that was started at 1000 s after RESET (blue curve). Figure 2(b) shows the resistance as a function of time after RESET from the same measurement (also blue curve). A drift coefficient $\alpha = 0.08$ was obtained. This measurement (blue curve) serves as a reference measurement.

After crystallization, the cell was RESET again and allowed to drift at 298 K for 1000 s. The cell is now subjected to a more complicated temperature-time profile (green curve in Figs. 2(a) and 2(b)). Instead of a continuous temperature ramp, a series of interrupted ramps were applied (each with 10 K/min). Each subsequent temperature ramp had a higher peak temperature and after each ramp, the temperature was returned back to 298 K.

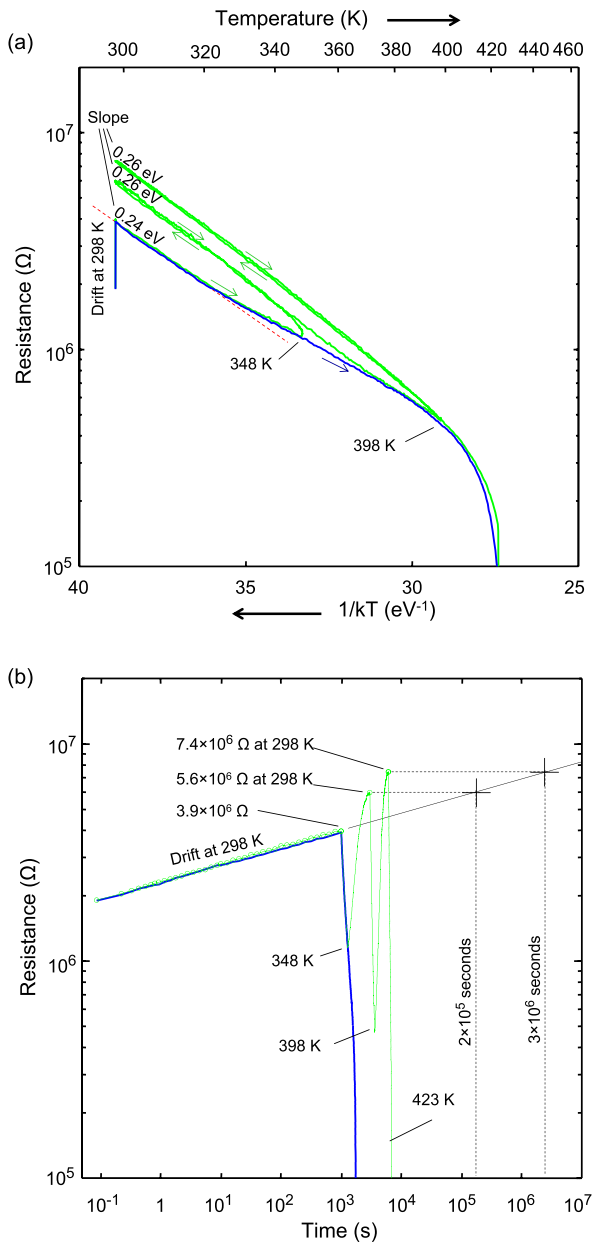

FIG. 2. Cell resistance as a function temperature (a) and time (b) for a PRAM line cell switched to the amorphous state at 298 K. The blue line shows the cell being crystallized by a single uninterrupted temperature ramp initiated 1000 s after RESET. At 298 K, the cell was RESET again and a series of temperature ramps were applied with peaks at 348 K, 398 K, and 423 K and each time cooling down to 298 K (green curves). The elevated temperatures experienced during the ramps accelerated the resistance drift compared to the drift at 298 K.

The first ramp had a peak of 348 K. It can be observed in Fig. 2 that this interrupted curve overlaps with the previous uninterrupted curve up to this peak temperature. This shows the excellent reproducibility of the measurement, because up to this point, the time and temperature profiles were exactly the same. The slope at the start of the ramp has a value of 0.24 eV and, as also observed in Fig. 1(b), the resistance curve shows evidence of drift as the temperature reaches 348 K shown by the slight increase of the resistance at the peak temperature.

Directly after reaching 348 K, the temperature was decreased back to 298 K. The slope of the descending temperature ramp equals 0.26 eV, notably different from the previous ascending ramp.

Directly after the previous resistance measurement at 298 K, the temperature is brought back up to 348 K (Fig. 2(b)). Now the cell resistance follows exactly the same values of the previous descending curve except for the temperature just below the former peak temperature of 348 K (Fig. 2(a)). Clearly, the cell properties have not been changed during the ramp down followed by a ramp up. As the temperature is further increased close to 348 K and beyond, the R(T) curve starts to resemble the uninterrupted (blue) curve. The same heating-cooling cycle is repeated with a next peak temperature of 398 K and in principle shows similar behavior as for the peak temperature of 348 K. The slope of 0.26 eV is roughly the same when descending from 398 K. The resistance, though, is at a higher absolute level than for the previous cooling curve after annealing only up to 348 K. During a final ramp to 423 K, the cell is eventually crystallized.

In summary, Fig. 2(a) shows that the resistance curve during each cooling ramp is reproduced during the directly following heating ramp. This is important, because it shows that a time-independent slope of log(R) versus 1/kT can be obtained, which can be considered a physically relevant measure of E_A. As the ramp is increased beyond the previous maximum temperature, the resistance curve (green) resembles the one for the single uninterrupted ramp (blue), and we again enter a region where the slope becomes time dependent, because it is affected by additional drift.

The cell resistance at a constant temperature increases in time by the well-established power law dependence.[2] Fig. 2(b) shows that after each interrupted ramp, the resistance at 298 K has been increased more than what would be expected from the extrapolated power law dependence (black line). Clearly, the temperature ramps accelerated the drift. The resistance at 298 K after a heating-cooling cycle with a peak at 348 K and 398 K was measured at 3.0×10^3 s and 6.1×10^3 s, respectively, after the RESET pulse (Fig. 2(b)). But the cell resistance at 298 K increased from 3.9×10^6 Ω just before the first cycle to 5.9×10^6 Ω after the first cycle and 7.4×10^6 Ω after the second cycle. Fig. 2(b) indicates that these resistance values are the equivalent of a continuous

uninterrupted drift at 298 K of 2×10^5 s (more than two days) and 3×10^6 s (five weeks), respectively. The heating-cooling cycle to 398 K thus increased the (equivalent) drift time by a factor of 500.

The values of E_A after the ramps to 348 K and 398 K remained rather constant even though the resistance at 298 K did increase due to drift by a factor of 1.5. The relation between the amorphous resistance at 298 K and E_A is further investigated with a more elaborate measurement.

A PRAM cell was brought to the amorphous state and the resistance was measured at 298 K for 20 s. Figures 3(a) and 3(c) show the resistance as a function of temperature and time, respectively (blue curve). Figure 3(c) shows the first 20 s after RESET plotted on a double-logarithmic scale to show that the cell follows the power law for two orders of magnitude in time. A drift coefficient of $\alpha = 0.09$ was obtained. Then the temperature was increased with a 10 K/min ramp rate until the cell crystallized (blue line). Fig. 3(a) shows that as the temperature increases, the resistance decreases first with a slope of 0.12 eV (to 303 K) and above 313 K with a slope of 0.19 eV.

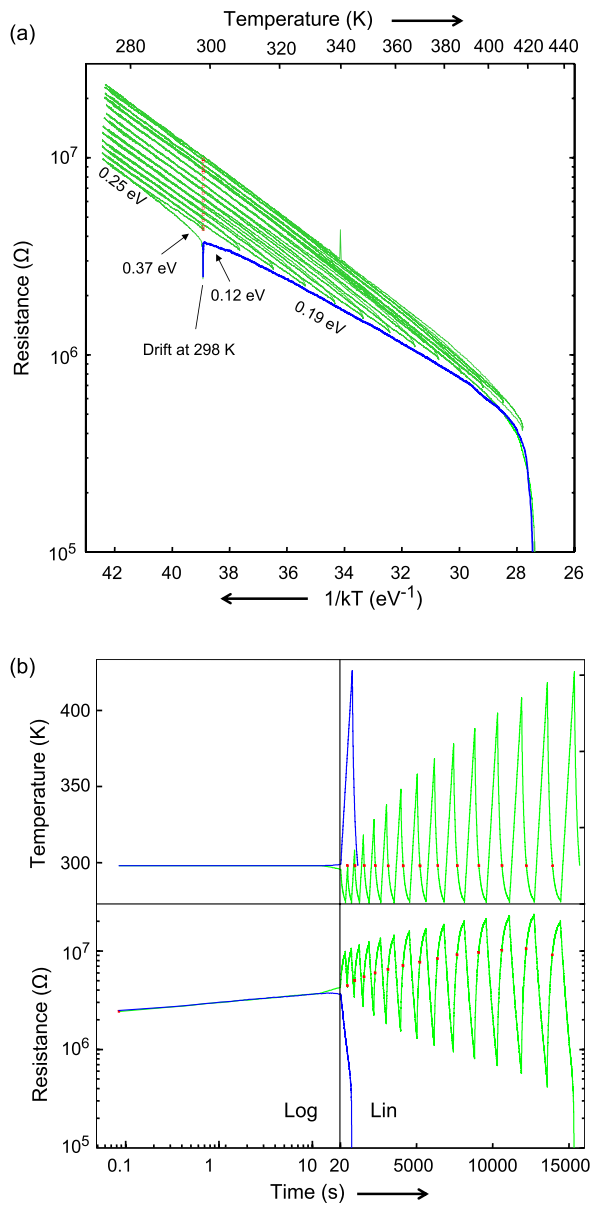

FIG. 3. Cell resistance as a function temperature (a) and time (b) for a PRAM line cell switched to the amorphous state at 298 K. The blue line shows the cell being crystallized by a single uninterrupted temperature ramp initiated 20 s after RESET. At 298 K, the cell was RESET again and after 20 s, the temperature was lowered to 276 K. A series of temperature ramps were applied with a peak at 298 K, 308 K, etc. and each time cooling down to 276 K (green curves). The red dots in (a) and (b) indicate the resistance at 298 K obtained during the ramp after each peak.

Next, the cell was RESET again at 298 K and after the cell drifted for 20 s, the temperature was decreased to 276 K. As the temperature decreases, the resistance initially has a slope of 0.37 eV and below 290 K has a slope of 0.25 eV. As mentioned above, this apparent discrepancy can simply be explained by drift still occurring during both ramps leading to increased or decreased values for the slope depending on the ramp direction, i.e., either cooling or heating, respectively. In the previous measurements (cf. Fig. 2), before any annealing cycle, the device was allowed to drift at room temperature for 1000 s; sufficiently long that a subsequent decrease in temperature would not cause observable influence of drift on the resistance. However, since in this experiment only 20 s of drift was allowed prior to the temperature cycle, a reduction in temperature still shows initially a behavior influenced by drift, as can be observed from the first part of the green curve in Figure 3(a) (i.e., the blue and green curves have clearly different initial slopes at 298 K).

Subsequently, starting from 276 K, a series of heating-cooling cycles with a peak at 298 K, 308 K, etc. were applied while the cell resistance was measured. Figure 3(a) shows the resistance as a function of temperature. The red data points in Figs. 3(a) and 3(c) correspond to the resistances at 298 K.

Due to the constant heat flow between the temperature stage and the liquid nitrogen reservoir and the heat capacitance of the copper heat conductor (not present during the measurements shown in Figs. 1 and 2), a small but significant discrepancy exists between the cell temperature and the measured temperature. The temperature shown in Fig. 3 was compensated for this effect by a thermal capacitive model on the basis of the evidence of Fig. 2 allowing for a maximum correction of 1 K.

From Fig. 3(a), values of the activation energy were obtained from the (time-independent) slopes of the temperature curves. Each data point represent a measurement performed *after* the indicated peak anneal temperature in the temperature range *below* 298 K. The obtained activation energies are shown as a function of the previously experienced peak anneal temperature in Fig. 4 together with a fit to the data. Also, Fig. 4 shows the resistance measured at 298 K plotted as a function of the (previously experienced peak) anneal temperature. Figs. 3 and 4 show that the resistance at 298 K as well as the activation energy increase slightly due to the application of the temperature ramps each time to a higher maximum temperature. The resistances measured at 298 K after annealing to the highest temperatures were probably due to partial crystallization. Along with the experimental results, simulated resistance and activation energy are plotted in Fig. 4 (red line). The applied model explaining the increase of R* and E_A will be discussed in Sec. IV.

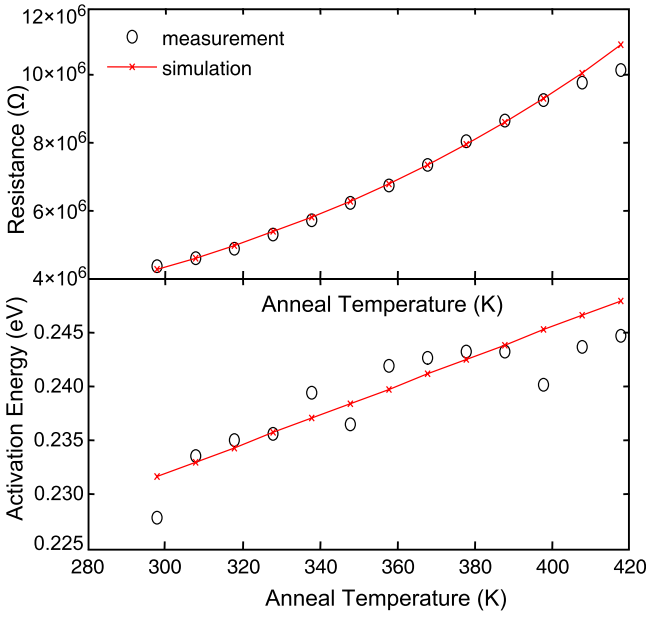

FIG. 4. Resistance measured at 298 K and activation energy E_A extracted from the cooling ramps in Fig. 3 below 298 K (black circles). The anneal temperature on the horizontal axis refers to the maximum temperature that has been reached *prior to* the measurement at and below 298 K, Both resistance and activation energy at 298 K increase upon drift due to the temperature dependence of the activation energy. The simulation reproduces this behavior (red line).

IV. DISCUSSION

Different physical interpretations of the nature of charge conduction and drift of the amorphous phase are proposed in literature.[2,4,5,8,18] Assuming that the electrical transport of phase change materials can be described with semiconductor behavior,[2,8,13] the resistance can be written as

$$R = R^* \cdot \exp\left(\frac{E_A}{kT}\right). \quad (1)$$

The activation energy E_A, typically assumed to be a temperature-independent constant, is roughly half the optical band gap E_g.[20] Therefore, it is commonly assumed that the Fermi level E_F is pinned in the middle of the band gap. For hole transport, electrons need to be activated from the band edge at $E_v = 0$ to above the Fermi level leaving holes behind and the activation energy can be written as

$$E_A = E_F - E_v = \frac{E_g}{2}. \quad (2)$$

Varshni found a general empirical law for the temperature dependence of the optical band gap in semiconductors with α, β, and E_0 being empirical parameters[21]

$$E_g = E_0 - \frac{\alpha T^2}{T + \beta}. \quad (3)$$

For various phase change materials, it has been shown experimentally that they follow a simplified version of this law[22,23]

$$E_g = E_0 - \xi T^2. \quad (4)$$

TABLE I. Parameters used in the simulation of the temperature dependent resistance. The parameters are chosen to reasonably fit the experimental data. E_0 is lower than for GeTe or $Ge_2Sb_2Te_5$ because the optical band gap of doped SbTe compounds is lower.[26,27] The temperature dependence of the band gap ξ is assumed to be in the same range as for other phase change materials and the pre-exponential factor R* is adjusted in order to account for the device geometry. The band gap increase is chosen to be just slightly higher than experimentally observed for GeTe.

R*	$1 \times 10^4\ \Omega$
E_0	0.39 eV
ξ	0.9 μeV/K^2
$E_0(T_a = 418\,K)/E_0(T_a = 298\,K)$	$1 + 0.12$
$\xi(T_a = 418\,K)/\xi(T_a = 298\,K)$	$1 - 0.12$

Typical values for E_0 and ξ for amorphous phase change materials like GeTe and $Ge_2Sb_2Te_5$ are about 0.9 eV and 1.3 μeV/K^2, respectively. Clearly, this temperature dependence needs to be taken into account when calculating resistances using Eqs. (1) and (2).

Furthermore, it has been shown that after accelerated drift by annealing, the band gap is increased,[12,24] while the shape of the temperature dependence is preserved.[25] In particular for GeTe, an increase of the band gap upon annealing at 413 K by about 9% has been measured.[25]

Based on these findings, the temperature dependent resistance shown in Fig. 3(a) has been modeled using Eqs. (1), (2), (4) and the parameters of Table I.

The temperature dependence of the band gap for annealing temperatures from 298 K to 418 K is shown in Figure 5. The lowest (blue) curve corresponds to the temperature dependence right after RESET at 298 K. The highest (red) curve corresponds to the temperature dependence of the band gap after the device has drifted at 418 K (and thus has

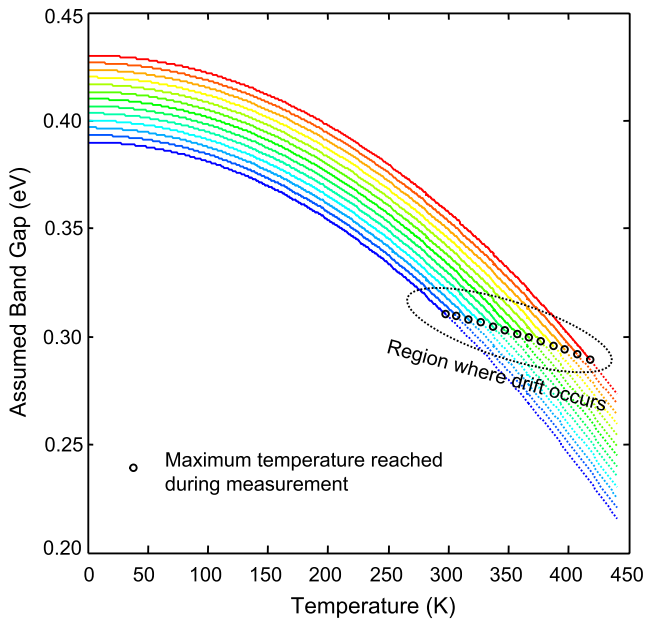

FIG. 5. The lowest (blue) curve corresponds to the temperature dependence right after RESET at 298 K. The highest (red) curve corresponds to the temperature dependence of the band gap after the device has drifted at 418 K leading to an assumed increase of the band gap by 12%. The intermediate curves correspond to 10 K steps in the interval 298–418 K.

obtained a frozen-in drift state for temperatures lower than 418 K) leading to an assumed increase E_0 by 12% and an assumed decrease of ξ by 12%. Between the initial band gap after RESET and the maximum band gap increase, a linear increase of the band gap with annealing temperature is assumed as a first order approximation. The intermediate curves correspond to 10 K steps in the range between 298 K and 418 K, where it is assumed that the drift after each increase of 10 K leads to a change of the band gap parameters by 1%. This way, the band gap is increased while the shape of its temperature dependence is preserved after drift at the various annealing temperatures. As indicated, each curve in principle only holds for a temperature lower than its corresponding annealing temperature, because only then additional drift can be neglected.

Calculating the resistance using this temperature dependent band gap after different sequential annealing steps yields the resistances shown in the lower panels of Figure 6. For comparison, the experimental data from Fig. 3 are plotted in the upper panels using identical x- and y-scales.

As Figure 6(a) shows, the absolute resistance as a function of temperature is matched correctly and also the increase of resistance can be explained quite accurately by an increase of the band gap by 12%. Not obvious in Fig. 6(a), Figure 6(b) reveals that all curves deviate significantly from a strict Arrhenius behavior. This is a natural consequence of the temperature dependence of the band gap and, thus, activation energy.

As shown in Figure 5, around 298 K, the temperature dependence is linear (to a first approximation) following roughly $E_g/2 = E_A = E_0 - \gamma T$. Inserting this into (1) yields

$$R = R^* \cdot \exp\left(\frac{E_A}{kT}\right) \approx R^* \cdot \exp\left(\frac{E_0 - \gamma T}{kT}\right)$$
$$= R^* \cdot \exp\left(-\frac{\gamma}{k}\right) \cdot \exp\left(\frac{E_0}{kT}\right). \quad (5)$$

Therefore, the temperature dependence of the activation energy around room temperature results in a decrease of the pre-exponential factor R* by $\exp(-\gamma/k)$. Furthermore, the slope of the Arrhenius plot shows an activation energy that is higher than the difference between E_f-E_v. In our case, the real activation energy for holes E_f-E_v at room temperature equals $E_g/2 = 0.15$ eV (see Fig. 5) while the slope of the Arrhenius plot yields roughly 0.23 eV (Fig. 4). To keep the model simple, the activation energy was assumed to be equal to half the band gap which is not necessarily the case. However, a natural consequence of the temperature dependence of the band gap is that the measured activation energy appears to be larger than the true activation energy. This is true regardless of the position of the Fermi level within the band gap.

This explains also why phase change materials typically are p-type even though the measured activation energy is half the optical band gap suggesting that the Fermi level is as close to the conduction band edge as to the valence band edge. In reality, the Fermi level is pinned closer to the valence band edge and only because of the temperature dependence, the activation energy appears to be larger. This demonstrates how dangerous it is to neglect the temperature dependence of the band gap for modeling electrical transport behavior as it is common practice.

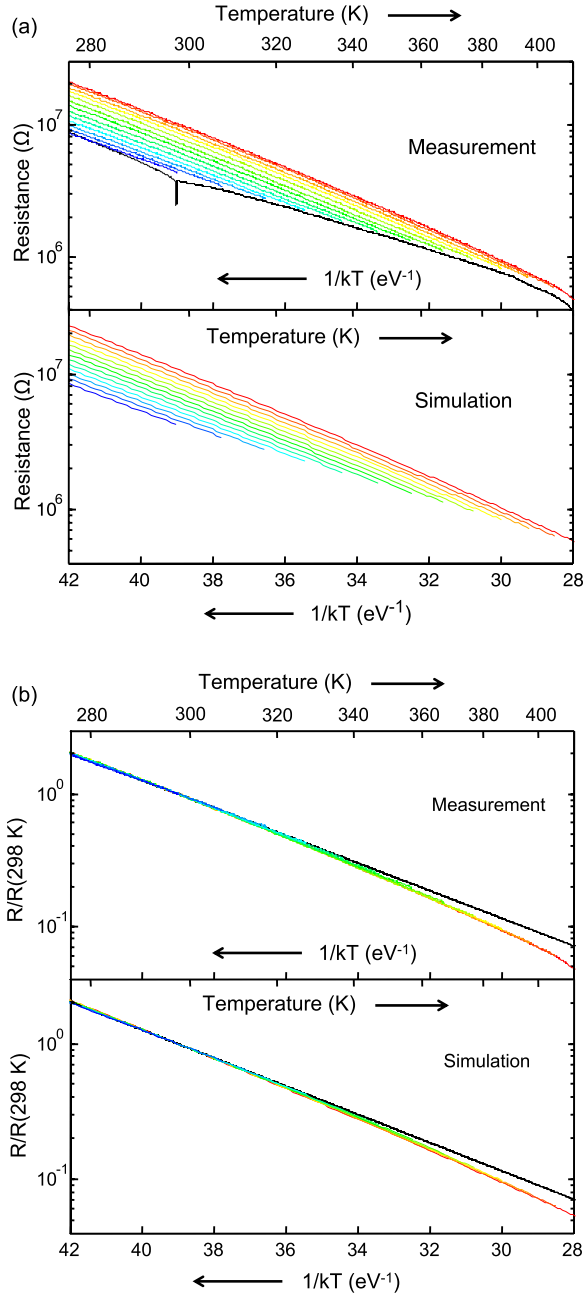

FIG. 6. Comparison of measurement and simulation of the absolute (a) and normalized (b) resistance of a device annealed to increasingly higher temperatures after RESET. The measurement data are identical to the once plotted in Figure 3. The color code indicates the maximum annealing temperature the device was exposed to. The black lines in (b) are calculated from temperature independent activated behavior with an activation energy of $E_A = 0.24$ eV plotted for reference.

Since the temperature dependence of the activation energy leads to a contribution in R* as well as the measured activation energy (slope of the Arrhenius plot), the increase of E_g upon annealing leads to an increase in both R* as well as E_A. The increase of those parameters upon annealing determined from the simulation is plotted alongside the experimental results as red lines in Figure 4. The nice match demonstrates that the typical temperature dependence of the

band gap explains the unexpected behavior naturally without any artificial assumptions.

V. CONCLUSIONS

When a phase-change memory cell is brought to the amorphous state and the temperature is increased by various fixed rates, the resistance is not a uniquely defined function of temperature (cf. Fig. 1(b)). In fact, resistance drift will occur during the temperature ramp, which will lead to a dependence of the resistance on the ramp rate. Lower ramp rates will allow more time for drift and lead to a higher resistance (R) at a specific temperature (T). In addition, by raising the cell temperature, the effect of drift is accelerated. As drift progressively takes place during the measurement (i.e., temperature ramp), the activation energy for conduction (E_A) as based on the slope of R versus T is underestimated. Therefore, E_A cannot be obtained by increasing the temperature without properly taking resistance drift into account. In contrast, when the cell is cooled down, additional temporal drift does not occur at these lower temperatures and only then a time-independent slope of log(R) versus 1/kT can be obtained, which can be considered a physically relevant measure of E_A.

For doped SbTe, we showed that a ramp up to 413 K and cooling back to room temperature accelerates drift by a factor of 500 with respect to drift solely at room temperature. The activation energy of conduction and pre-exponential factor was measured as a function of annealing temperature (based on the time-independent slope of log(R) versus 1/kT due the absence of additional drift below the annealing temperature). An increase of both parameters was observed and all the experimental results were reproduced excellently on the basis of a theoretical model that takes the temperature dependence of the optical band gap into account. According to our model, the change of the optical band gap with changing temperature does not alter after various annealing temperatures from room temperature up to 418 K, but annealing increases the absolute value of the band gap by 47 meV. Still it has to be emphasized that the temperature dependence of the optical band gap has to be taken into account; neglecting it leads to a significant overestimation of the values derived for the optical band gap and pre-exponential factor.

ACKNOWLEDGMENTS

The research was carried out under Project No. MC3.05241 in the framework of the Strategic Research program of the Materials innovation institute M2i. Financial support from the M2i is gratefully acknowledged. M.S. acknowledges funding by DFG through the collaborative research centre SFB 917 Nanoswitches.

[1]S. Raoux, Annu. Rev. Mater. Res. **39**, 25 (2009).
[2]A. Pirovano, A. L. Lacaita, F. Pellizzer, S. A. Kostylev, A. Benvenuti, and R. Bez, IEEE Trans. Electron Devices **51**, 714 (2004).
[3]J. L. M. Oosthoek, K. Attenborough, G. A. M. Hurkx, F. J. Jedema, D. J. Gravesteijn, and B. J. Kooi, J. Appl. Phys. **110**, 024505 (2011).
[4]I. V. Karpov, M. Mitra, D. Kau, G. Spadini, Y. A. Kryukov, and V. G. Karpov, J. Appl. Phys. **102**, 124503 (2007).
[5]M. Mitra, Y. Jung, D. S. Gianola, and R. Agarwal, Appl. Phys. Lett. **96**, 222111 (2010).
[6]S. Braga, A. Cabrini, and G. Torelli, Appl. Phys. Lett. **94**, 092112 (2009).
[7]D. Ielmini, A. L. Lacaita, and D. Mantegazza, IEEE Trans. Electron Devices **54**, 308 (2007).
[8]M. Boniardi, A. Redaelli, A. Pirovano, I. Tortorelli, D. Ielmini, and F. Pellizzer, J. Appl. Phys. **105**, 084506 (2009).
[9]Y. Yin, T. Noguchi, H. Ohno, and S. Hosaka, Appl. Phys. Lett. **95**, 133503 (2009).
[10]T. Nirschl, J. B. Phipp, T. D. Happ, G. W. Burr, B. Rajendran, M. H. Lee, A. Schrott, M. Yang, M. Breitwisch, C. F. Chen, E. Joseph, M. Lamorey, R. Cheek, S. H. Chen, S. Zaidi, S. Raoux, Y. C. Chen, Y. Zhu, R. Bergmann, H. L. Lung, and C. Lam, in *Write Strategies for 2 and 4-bit Multi-Level Phase-Change Memory* (IEEE, Washington, DC, 2007), p. 461.
[11]D. Ielmini, S. Lavizzari, D. Sharma, and A. L. Lacaita, Appl. Phys. Lett. **92**, 193511 (2008).
[12]D. Krebs, R. M. Schmidt, J. Klomfaß, J. Luckas, G. Bruns, C. Schlockermann, M. Salinga, R. Carius, and M. Wuttig, J. Non-Cryst. Solids **358**(17), 2412 (2012).
[13]A. E. Owen and J. M. Robertson, IEEE Trans. Electron Devices **20**, 105 (1973).
[14]S. Privitera, C. Bongiorno, E. Rimini, R. Zonca, A. Pirovano, and R. Bez, Mater. Res. Soc. Symp. Proc. **803**, HH1.4 (2003).
[15]D. T. Castro, L. Goux, G. A. M. Hurkx, K. Attenborough, R. Delhougne, J. Lisoni, F. J. Jedema, M. Zandt, R. A. M. Wolters, D. J. Gravesteijn, M. A. Verheijen, M. Kaiser, R. G. R. Weemaes, and D. J. Wouters, "Evidence of the thermo-electric Thomson effect and influence on the program conditions and cell optimization in phase-change memory cells," Tech. Dig. – Int. Electron Devices Meet. **2007**, 315.
[16]D. Adler, H. K. Henisch, and N. Mott, Rev. Mod. Phys. **50**, 209 (1978).
[17]D. Ielmini, S. Lavizzari, D. Sharma, and A. L. Lacaita, "Physical interpretation, modeling and impact on phase change memory (PCM) reliability of resistance drift due to chalcogenide structural relaxation," Tech. Dig. – Int. Electron Devices Meet. **2007**, 939.
[18]D. Ielmini and Y. Zhang, J. Appl. Phys. **102**, 054517 (2007).
[19]J. Oosthoek, B. J. Kooi, J. T. M. De Hosson, D. Gravesteijn, K. Attenborough, R. Wolters, and M. Verheijen, "Crystallization studies of doped SbTe phase-change thin films and PRAM line cells: Growth rate determination by automated TEM image analysis," in *Proc. E/PCOS Symp.* (2009), p. 140.
[20]A. Pirovano, A. L. Lacaita, A. Benvenuti, F. Pellizzer, and R. Bez, IEEE Trans. Electron Devices **51**, 452 (2004).
[21]Y. P. Varshni, Physica **34**, 149 (1967).
[22]J. Luckas, S. Kremers, D. Krebs, M. Salinga, M. Wuttig, and C. Longeaud, J. Appl. Phys. **110**, 013719 (2011).
[23]S. Kremers, "Optical properties of phase change materials for novel optical and electrical storage applications," Ph.D. dissertation (RWTH Aachen University, 2009).
[24]P. Fantini, S. Brazzelli, E. Cazzini, and A. Mani, Appl. Phys. Lett. **100**, 013505 (2012).
[25]J. Luckas, "Electronic transport in amorphous phase-change materials," Ph.D. dissertation (RWTH Aachen University, 2012).
[26]J. K. Olson, H. Li, T. Ju, J. M. Viner, and P. C. Taylor, J. Appl. Phys. **99**, 103508 (2006).
[27]E. Prokhorov, A. Mendoza-Galván, J. González-Hernández, and B. Chao, J. Non-Cryst. Solids **353**, 1870 (2007).